Dynamic Droop Control Method for Islanded Photovoltaic Based Microgrid for Active and Reactive Power Control with Effective Utilization of Distributed Generators

Urvi N. Patel*‡, Hiren H. Patel**

*Research scholar, Electrical Engineering Department, Gujarat Technological University, Chandkheda, Ahmedabad, Gujarat, India.

**Department of Electrical Engineering, Sarvajanik College of Engineering and Technology, Athwalines, Surat, Gujarat,

(urvip3004@gmail.com, hiren.patel@scet.ac.in)

‡Corresponding Author; Urvi N. Patel, Research scholar, Electrical Engineering Department, Gujarat Technological University, Chandkheda, Ahmedabad, Gujarat, India., Gujarat, India, urvip3004@gmail.com

Abstract- Conventional droop-control scheme shares the load amongst energy sources in proportion to their ratings. The scheme suffers from the issue of ineffective utilization of the sources when performance of some of the sources is dependent on environmental conditions. Hence, a modified droop-control strategy is proposed for a microgrid comprising of photovoltaic (PV) based distributed generators (DG) operating in parallel with other DGs. Dynamic nature applied to the droop characteristic by the primary control unit (PCU) sets the frequency reference such that the PV sources operate at their maximum power point and the energy demanded from the auxiliary source is the minimum. The margin available after supplying the active power is used to allocate the references for reactive power sharing. The reactive power sharing algorithm employed in secondary control unit (SCU) ensures that the standard deviation of the percentage utilization of the inverters is kept the minimum. Even in case of the failure of the communication between the PCU and SCU, a reasonably good performance is ensured as the control shifts to the master-slave control having dynamic droop adjustment feature. The effectiveness of the proposed strategy against other approaches is justified through the simulation results obtained in MATLAB/Simulink.

Keywords- Microgrid, Droop control, Photovoltaic, Active power sharing, Reactive power sharing.

1. Introduction

Photovoltaic (PV) is widely used as distributed generation (DG) source in a microgrid (MG). However, PV connected MG faces several challenges due to the uncertain and intermittent nature of PV [1]. Due to lesser inertia and unavailability of relatively stable voltage and frequency references, the islanded mode of MG presents more challenges [2].

Many issues like voltage and frequency deviation, power unbalance, overloading of certain sources, circulating currents etc. in the islanded MG can be addressed to a certain extent by accurate sharing of active power (P) and reactive power (Q) amongst the DGs. The droop control method, which employs active power versus frequency (P-ω) and reactive power versus voltage (Q-V) relation for active and reactive power sharing amongst the DGs of the MG respectively, is quite popular as it does not require any communication link between DGs [3-5]. However, the conventional P-ω droop method shares active power based on fixed droop coefficient irrespective of available energy from nonconventional energy sources like PV and wind [6-8]. Hence, the frequency and the voltage set points are mainly determined by the load and it ignores the variation in P due to the intermittent and uncertain nature of the energy source. With the conventional droop control, a drop in generation of one PV based DG causes reduction in output of other DGs operating in parallel. This requires auxiliary source (AS) with large capacity to maintain power balance and stability. To overcome this limitation a dynamic active power sharing is proposed which is detailed in

the section 3.1.

Droop control methods [9-12] have also been studied with a view to improve the performance in terms of improved stability, accuracy in power sharing, minimization in voltage and frequency errors etc. But in most of the research, the PV source is modeled as a constant voltage source and/or is not always operated corresponding to maximum power point. In [13] dynamic droop load sharing is proposed, wherein the insensitivity of the conventional droop control is modified by incorporating dynamic droop parameters. However, PV source is not operated at the MPP and its effectiveness for various load conditions is not explored. An enhanced droop control, which shares active power amongst paralleled two-stage PV inverters by varying the dc link voltage within a reasonable range, is reported in [14]. However, the absence of storage may result into instability, especially when operating with low irradiation level or with rapidly varying load. Unlike the above the proposed approach the proposed dynamic droop based control ensures that the PV sources are effectively utilized (i.e. always operated at the maximum power point (MPP)) and the auxiliary source supplies the minimum amount of energy to avoid any instability due to the power balance.

Besides the active power exchange, the PV inverters must be controlled to deliver reactive power so that the inverters are optimally utilized. *Q-V* droop control is quite popular for sharing the reactive power amongst the DGs. But the accuracy with which the reactive power is shared is greatly influenced by the mismatch of the impedance of the DG feeders, imbalance in the load, non-linear loads etc. Various strategies have been reported for reactive power sharing to tackle such issues [15-17]. However, only few studies have reported reactive power sharing based on effective use of the reactive power margin of the inverter available after meeting the active power demand. Equal reactive power sharing [ERPS] algorithm based droop control method [18], which shares reactive power demand equally amongst the inverters irrespective of variation in active power, results into unequal utilization of inverters. Some of the inverters may even get overloaded. Hence, it is important to consider this aspect, especially for the PV based DGs where the active power supplied through the inverter is dependent on the environmental conditions. A quasi-master-slave control approach [19], where the dispatchable source (storage) based DGs are used as master and the non-dispatchable source based DGs (e.g. PV based DGs) slaves, employs the adaptive droop-settings for reactive (and active) power control to adjust with the varying environmental conditions.

The droop control based reactive power sharing algorithm presented in [20] also considers the variation of active power while sharing reactive power amongst the inverter. The algorithm is executed by the secondary control unit that provides reactive power references for the *Q-V* droop setting. This prevents overloading of inverter. However, it requires communication channel and the effective utilization of the inverters is not ensured. An optimal reactive power strategy (ORPS) to share reactive power in proportion to active power delivered by inverter is proposed in [21]. But, with ORPS control when the active power delivered by the PV based DGs

differ greatly, some of the DGs operate near to their rating while others may be under-utilized. To overcome this limitation, equal apparent power sharing (EAPS) strategy is preferred [22], which equalizes the apparent power of all DGs. However, EAPS works effectively only for equal rating DGs. The modified EAPS algorithm presented in [23], considers the best order in which the reactive power must be calculated for assigning the reference reactive powers to the parallel connected inverters. It obtains the solution that provides the least standard deviation (LSD) of the utilization factors of the inverters. The method is accordingly termed as EAPS-LSD. The variation in the utilization factors of the inverters can further be minimized if the inverters share the apparent power in proportion to their rating. In this respect, the proportional apparent power sharing (PAPS) algorithm, which is detailed in section 3.2, is presented to share reactive power in proportion to available apparent power rating of the DGs. It helps in minimization of the standard deviation of the utilization factors of the inverters.

Thus, the paper presents modified droop control method to share active and reactive power amongst DGs. The salient features of the proposed method are summarized as under:

1. Dynamic droop characteristics applied through the primary control unit (PCU) ensures that the PV based DGs are always operated at their MPP, while other DGs share active power in proportion to their ratings.

2. The AS provides the active power only when all DGs hit their limits. This minimizes the AS requirement.

3. Reactive power is shared amongst the PV inverters in relation to the actual active power generated by them.

4. The reactive power sharing algorithm employed in the secondary control unit (SCU) ensures that the standard deviation of the percentage utilization of the inverters is kept the minimum.

5. In case of the communication failure between the primary and the secondary control units, the DGs fall back on the master-slave control approach employing dynamic *P-ω* and *Q-V* droop control.

The rest of the paper is organized as follows. Section 2 presents a microgrid comprising of PV based DGs and other DGs considered for the study while section 3 details the control scheme used to share the active and reactive power control amongst the DGs and to have the effective utilization of the all the resources. Simulation results for the conventional methods and the proposed approach are presented in section 4 which is followed by some important conclusions in section 5.

2. System Configuration

The system configuration comprising of four DGs and the auxiliary energy source shown in Fig. 1(a), is considered to evaluate the performance of the proposed modified droop control strategy. The block diagram shown in Fig. 1(b) shows the control unit comprising of PCUs and the SCUs. The control scheme is detailed in the section 3.

(a)

(b)
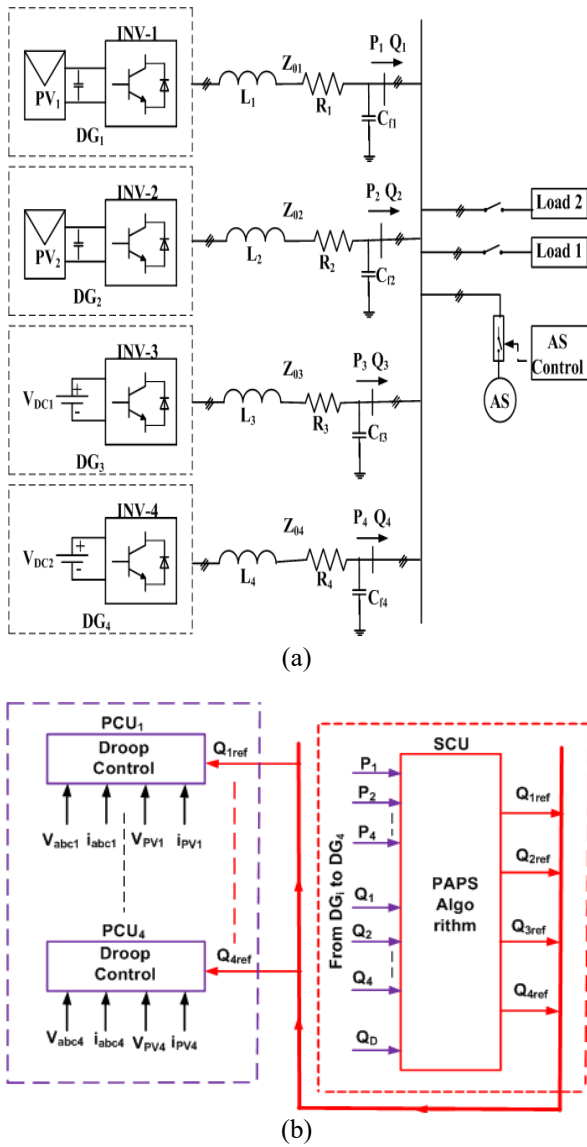
Fig. 1. Microgrid with four DGs:
 (a) System Configuration and (b) Control block diagram

The first two DGs (DG$_1$ and DG$_2$) are the photovoltaic based DGs while the remaining two (DG$_3$ and DG$_4$) are fed from reliable energy source like microturbines or fuel cell. The PV based DGs (DG$_1$ and DG$_2$) are considered to be identical. The PV based DGs comprises of a PV array along with a dc-dc converter, which is controlled to output maximum power using MPP tracking (MPPT) method. It is not shown in Fig.1 for the sake of brevity. The power electronic converters (inverters 1 through 4) are used to control the energy supplied by these DGs. Additionally they are also controlled to provide the reactive demand of the load. The impedances Z_i, where 'i' represents i^{th} DG, take into account the impedance of interfacing inductor, the impedance of cable and isolation transformer.

An auxiliary source represented by AS is required to satisfy power balance. It comes into action and supplies the power when load demand increases beyond the cumulative active power generated by all the DGs. It acts as a recipient of active power in case the active power required by the load is less than that generated by the PV based DGs. The AS also participates in the active power exchange when a sudden change in the load or input power occurs. Once the control algorithm regains the new equilibrium position (i.e. power balance is regained) the power supplied/absorbed by AS becomes zero.

Amongst four DGs, the reliable sources based DGs (DG$_3$ and DG$_4$) are operated with conventional P-ω droop control while environment dependent PV source based DGs (DG$_1$ and DG$_2$) are controlled with modified P-ω droop control method for supplying the active power. As the active power supplied by the PV based DG vary with the environmental conditions, the maximum reactive power which can be exchanged through its inverter also varies. The control scheme employed takes care of variable reactive power margin of the PV based inverters. The PAPS reactive power algorithm executed by the SCU assigns reactive power references to PCUs of inverters 1 through 4. These references finally set the reactive power of the inverters in proportion to the available reactive power capabilities of these inverters.

3. Proposed control scheme for DG

The principles of modified active power droop control and reactive power control is first explained in this section and then the detailed control scheme is presented.

3.1 Principle of Modified Active Power Droop Control

The principle of modified active power droop control is illustrated through Fig.2, which shows P-ω characteristics for DG$_1$- DG$_4$. The droop characteristics are defined in general for these sources as

Where m is the slope of the characteristic; ω_o is the

$$\omega = \omega_o - m(P_{rat} - P_o) + x(K_p + \frac{K_i}{s})(P_{Mpp} - P_o) \quad (1)$$

$$m = \Delta\omega / P_{rat} \quad (2)$$

frequency corresponding to rated power P_{rat} of the DG; P_{MPP} is maximum power supplied by PV sources, x is scaling factor and ω is the operating frequency when the DG supplies power P_o. For PV based sources P_{rat} represents the maximum active power that it provides when working under standard test conditions (STC) i.e. its nominal power rating.
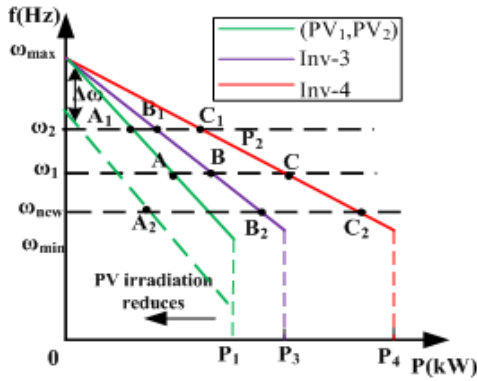
Fig.2. Modified active power-frequency droop characteristic

Let these PV based DGs are initially operating at frequency ω_1, corresponding to point A as shown in Fig.2. The operating points for the DG$_3$ and DG$_4$ at this frequency are B and C. If these DGs are controlled using conventional P-ω droop control, in case of the decrease in output power of PV based DGs (due to the decrease in insolation), the operating point on its droop characteristic shifts to A$_1$ corresponding to frequency ω_2 ($\omega_2 > \omega_1$). This in turn decreases the output power of DG$_3$ and DG$_4$ as they have to operate at the same frequency ω_2 (corresponding to points B$_1$ and C$_1$, respectively). This will lead to active power imbalance in the system. To avoid such situation, when the output of PV array decreases due to the decrease in the insolation, its operating frequency must be lowered (rather than increasing) so that the DG$_3$ and DG$_4$ can supply the extra power to maintain the equilibrium/stability. Thus, the modified droop characteristics exhibits the dynamic nature as the additional frequency component $(\Delta\omega)$ is added to the frequency set point of the conventional droop characteristic. As a result, the operation of both DG$_1$ and DG$_2$ occur corresponding to point A$_2$ (at ω_{new}) while the DG$_3$ and DG$_4$ operate corresponding to points B$_2$ and C$_2$, respectively. Detailed control scheme, which employs this principle of active power control, is discussed in sub-section 3.3 that describes the PCU.

3.2   Reactive Power Control

The principle of sharing apparent power among inverters with the proposed method is described using vector representation shown in Fig.3 for four inverters having S_{1N}...S_{4N} as their nominal apparent power ratings. Proportional apparent power sharing (PAPS) is based on the principle of operating the inverters in such a way that they share the apparent power in proportion to their nominal ratings.

The total desired apparent power (S_{TD}) depends on reactive power demand of the load (Q_D) and total active power (P_T) generated by the DGs and is represented as Eq. (3)

$$S_{TD} = \sqrt{P_T^2 + Q_D^2} \tag{3}$$

The active powers generated by PV arrays PV$_1$-PV$_2$ depends on environmental conditions experienced by these arrays. Hence, their active powers P_i may vary. Accordingly, the available reactive power capability of the inverters Q_i, also vary. The total reactive power capability available Q_T with the system comprising of k DGs is thus expressed as Eq. (4).

$$Q_T = \sum_{i=1}^{k} (Q_i) \tag{4}$$

Accordingly, the total apparent power capability of system S_T is expressed by Eq. (5)

$$S_T = \sqrt{P_T^2 + Q_T^2} \tag{5}$$
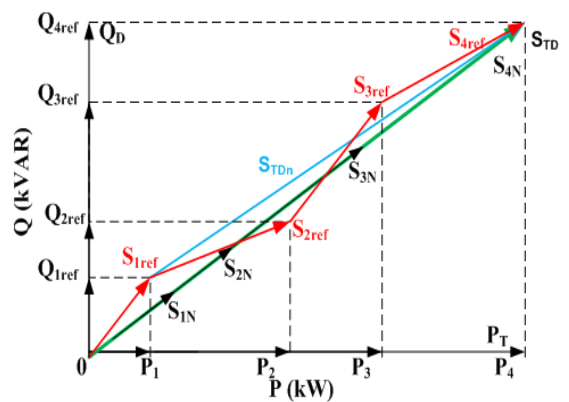
Fig.3. Vector representation of reactive power sharing with PAPS

As P_i (for PV based DGs) and hence, the Q_i vary with the change in environmental conditions, the reactive power must be shared such that the all the inverters operate at the equal percentage utilization. To achieve this, the desired apparent power (S_{TD}) must be shared amongst the inverters in proportion to their ratings. Hence, the reference apparent power (S_{1ref}) for the inverter 1 is obtained by Eq. (6)

$$S_{1ref} = \frac{S_{1N}}{S_T} \times S_{TD} \tag{6}$$

The reactive power reference Q_{1ref} for the inverter-1 is computed using Eq. (7)

$$Q_{1ref} = \sqrt{S_{1ref}^2 - P_1^2} \tag{7}$$

As observed from Fig.3, vector S_{1ref} is not aligned with S_{TD} and hence, the remaining apparent power S_{TDn} must now be supplied by inverters 2-4. As a result these three inverters are controlled to share the remaining apparent power in proportion to their ratings. Thus, inverter-2 must be assigned reference apparent power S$_{2ref}$ expressed by Eq. (8).

$$S_{2ref} = \frac{S_{2N}}{S_{Tn}} \times S_{TDn} \quad (8)$$

where S_{Tn} is the total of nominal apparent power ratings of the remaining inverters, which can be represented by Eq. (9) where S_{Tn} is the total of nominal apparent power ratings of the remaining inverters, which can be represented by Eq. (9)

$$S_{Tn} = \sqrt{(P_T - P_1)^2 + (Q_T - Q_1)^2} \quad (9)$$

On the similar lines, the reactive power references for the inverters 3 and 4 can be computed. Fig.3 shows reference apparent power (S_{iref}) of each inverter, which indicate that their vector length is proportional to their nominal ratings. Based on the above principle, a control algorithm is processed to determine the best possible alternative of distributing the reactive power amongst the inverters to achieve equal percentage utilization of the inverters. This algorithm is used in the SCU to compute the reference reactive power for the inverters.

The algorithm leads to nearly equal utilization of the inverters, which can be measured in terms of the standard deviation (SD) of the utilization factors. The utilization factor (UF) and the SD are expressed by Eqs. (10) and (11), respectively.

$$UF_i = S_{iref} / S_{iN} \quad (10)$$

$$SD = \sqrt{\frac{1}{(k-1)} \sum_{i=1}^{k} (UF(i) - UF_{mean})^2} \quad (11)$$

where UF_{mean} is the mean value of UF for all inverters ($i=1$ through k).

3.3 Inverter Control

Figure 4 shows in detail the block diagram of the PCU used for controlling the inverter's output voltage to achieve desired active and reactive power exchange. As observed through the Fig.4, the PCU incorporates the modifications in the conventional droop characteristics for sharing the active and reactive power of the load.

The inverter's output voltage (e_{abc}) and current (i_{abc}) are transformed into d-q frame to obtain the active power (p_0) and reactive power (q_0) using Eqs.(12) and (13)

$$p_o = 1.5(i_d V_{sd} + i_q V_{sq}) \quad (12)$$

$$q_o = 1.5(i_q V_{sd} - i_d V_{sq}) \quad (13)$$

where i_d, and i_q are d and q axis components of inverter's output current, respectively while V_{sd} and V_{sq} are d and q axis components of inverter's output voltage, respectively. Average values of active power (P_o) and reactive power (Q_o) is then derived using first order low pass filter as expressed by Eqs. (14) and (15), respectively.

$$P_o = \frac{\omega_c}{s + \omega_C} \times \frac{3}{2} (i_d V_{sd} + i_q V_{sq}) \quad (14)$$

$$Q_o = \frac{\omega_c}{s + \omega_C} \times \frac{3}{2} (i_q V_{sd} - i_d V_{sq}) \quad (15)$$

where ω_c represents cut-off frequency.

Modified active power droop control modifies P-ω characteristic represented by Eq. (1). The desired frequency (ω_{ref}) of the modified droop controller is obtained by adding a component $\Delta\omega$ to the frequency ω obtained from the conventional droop characteristic. For the PV based DGs, maximum power of PV corresponding to the STC is used for P_{rat} in Eq.(2) to derive ω. The error (ΔP) between the maximum power extracted from the PV array under given conditions (P_{MPP}) and the active power supplied through the inverter (P) is used to derive $\Delta\omega$. The P_{MPP} information is obtained from the perturb and observe (P&O) MPPT algorithm implemented with the first-stage (dc-dc) converter. ΔP is then scaled by a factor x represented by Eq.(16) before it is processed by the PI controller.

$$x = \Delta\omega / P_{MPP} \quad (16)$$

ω_{ref} required for the voltage control loop, is then derived as expressed by (17) using $\Delta\omega$ and ω.

$$\omega_{ref} = \Delta\omega + \omega \quad (17)$$

The reactive power droop control is implemented using reactive power vs. voltage (Q-V) droop equation represented by Eq.(18), which provides the reference voltage (V_{ref}) for the voltage control loop.

$$V_{ref} = V_o - n(Q^* - Q_o) \quad (18)$$

$$n = \Delta V / Q^* \quad (19)$$

The reference reactive power (Q^*) required for Eqs. (18)- (19) is obtained through the reactive power sharing algorithm (described in sub-section 3.2) executed by the SCU. In case the communication link between the PCUs and the SCU fails, the reactive power references are set by the master-slave control approach with the adaptive feature for both P-ω and Q-V droop. In such case the reactive power reference used in Eqs. (18)-(19) (for i^{th} inverter) is calculated from locally available data using Eq. (20).

$$Q^*_i = \sqrt{S_{iN}^2 - P_i^2} \quad (20)$$

Voltage and frequency references, V_{ref} and ω_{ref}, respectively, are then applied to voltage control loop. It includes reference sinusoidal generator and voltage regulator loop. Reference generator generates sinusoidal three-phase ac voltage from the V_{ref} and ω_{ref}, and then further applies abc-dq transformation to derive the reference d-q voltage components V_{d*} and V_{q*}. Voltage regulator loop compares these V_{d*} and V_{q*} with actual inverter output d-q voltage components (V_d and V_q). The error is then processed to derive the three-phase sinusoidal reference voltage signal for PWM control of the inverter. The control scheme for DG3 and DG4 are identical except that it does not incorporate MPPT algorithm and the blocks that derive $\Delta\omega$.
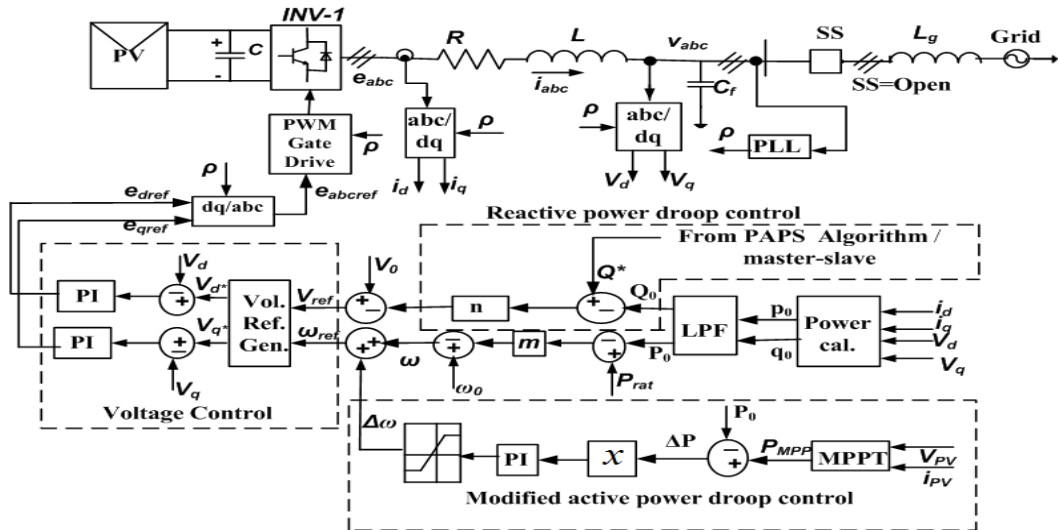
Fig. 4. Control circuit block diagram for PCU of the PV inverter

4. Simulation Results

To demonstrate the effectiveness of the proposed control strategy in sharing the active and reactive power amongst the various sources, the microgrid system shown in Fig. 1(a) is simulated in MATLAB/Simulink.

Table 1. Rating and parameters for the system of Fig.1

Parameters	Value
PV inverter-1 rating (S_1)	250 kVA
PV inverter-2 rating (S_2)	250kVA
Inverter-3 rating (S_3)	375kVA
inverter-4 rating (S_4)	565 kVA
Rating of AS	1000 kVA
Line impedance (Z_1,Z_2)	R_1=0.5Ω, L_1=320μH, C_1=20μF
Line impedance (Z_3)	R_3=0.33Ω,L_3=213μH,C_3=30μF
Line impedance (Z_4)	R_4=0.22Ω,L_4=142μH,C_4=45μF
m_1,m_2,m_3,m_4 (Hz/kW)	-2.5e-6,-2.5e-6,-1.6e-6,-.11e-6
n_1,n_2,n_3,n_4 (V/kVAR)	-1e-4,-1e-4,-6.66e-5,-4.44e-5
L-L voltage (rms)	415 V
Nominal frequency f(Hz)	50
Frequency range (Hz)	50.2-49.7

Table 2.Insolation and output power variation of PV

Time (s)	Insolation α_1kW/m^2	Output Power (kW)	Insolation α_2kW/m^2	Output Power (kW)
0-1	1.0	200	1.0	200
1-2	0.5	100	1.0	200
2-3	0.5	100	0.3	60

The performance of the proposed control strategy is also evaluated against other approaches [20], [21]. The system parameters considered for the simulation study are mentioned in Table 1 while Table 2 shows the variation in

the maximum power output of the PV arrays (PV$_i$) due to the variation in the insolation level (α_i).

Figure 5 shows results obtained with the conventional droop control method. The four DGs controlled using the droop control operates simultaneously to meet the demand of the 1000kVA, 0.8 pf (lag) load (i.e. 800kW, 600kVAR). It is observed from Fig. 5(a), that the active power supplied by the four DGs is in proportion to their ratings (250: 250: 375: 565 i.e. 1: 1: 1.5: 2.26). Thus, during t=0-1 s, active power supplied by the two PV sources is 140kW while that of the inverters 3 and 4 are 215kW and 312kW, respectively.
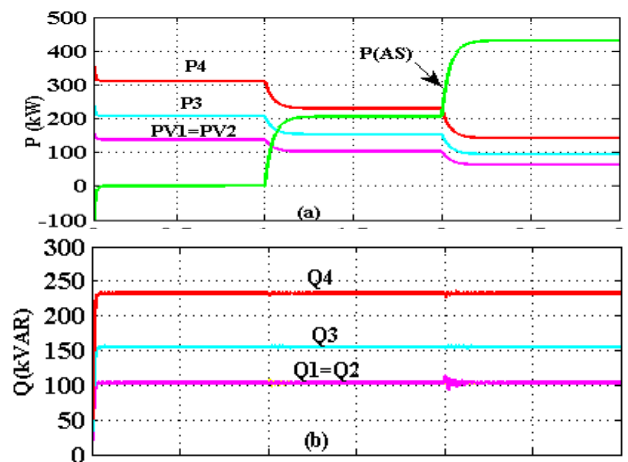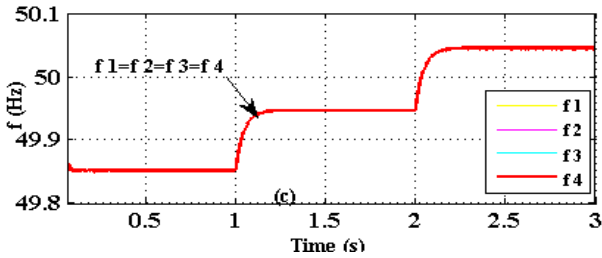
Fig. 5. Conventional droop control: (a) Active power sharing (b) Reactive power sharing(c) Frequency

Thus the ratio of the power shared amongst the DGs is 1: 1: 1.53: 2.23, which is in close approximation to the ration of the ratings of the inverters mentioned above. As the inverters are controlled to share the active power in proportion to the ratings of inverters, the power supplied through the PV based inverters is much less than the maximum power (200kW as shown in Table 2) that the PV sources can supply, leading to the ineffective utilization of the PV sources.

At t=1s as the insolation on the PV array PV_1 decreases to $0.5kW/m^2$, it can now supply only 100kW. As the droops of all the DGs are fixed in the conventional droop control, other sources (DG_2 through DG_4) are also forced to reduce their power to maintain the sharing of power in proportion to their ratings. Thus, the PV array of DG_2 which has the capacity to generate 200kW during t=1s-2s, is also constrained to supply only 100kW (equal to that of DG_1). The new equilibrium point is achieved by increasing the frequency as observed in Fig.5(c). The reduction in the insolation from $1kW/m^2$ to $0.3kW/m^2$ (at t=2s) on the PV array associated with the DG_2, further increases the frequency (Fig. 5(c)), thereby causing all other sources to decrease their output (Fig. 5(a)). This in turn forces the auxiliary source (AS) to generate more power to maintain the power balance. However, the change in the insolation does not affect the sharing of reactive power as observed from Fig. 5(b).

It can be observed that the reactive powers supplied by the inverter are also in proportion to the ratings of the inverters. The conventional droop control strategy is thus not able to achieve the effective utilization of the PV arrays as observed from the data tabulated in Table 3. The PV sources are underutilized for all the time intervals as observed from the active power of DG_1 and DG_2 mentioned in Table 3. These values are much lower than the power that the PV arrays can generate under different time intervals (as mentioned in Table 2).

Fig. 6 shows the simulation results with the modified P-ω control strategy, which always ensure the operation of the PV arrays at their maximum power points. It is observed from Fig.6 (a) that during t=0-1s, active power delivered by both PV sources is 200kW, which is the maximum power that the PV sources generate with insolation of 1 kW/m^2. This is obtained by inserting an additional frequency component $\Delta\omega$

to shift the P-ω characteristics. It is observed from Fig. 6(b) that the addition of $\Delta\omega$, changes the operating frequency to 49.95 Hz. Inverters 3 and 4 deliver active power according to their fixed droop setting, however, at new operating points that correspond to a new frequency. During t=1-2s, when the output power of PV_1 is reduced to half (100kW), $\Delta\omega$ causes the P-ω characteristic of inverter-1 to change such that the operating frequency decreases, unlike conventional droop control where the frequency increases as shown in Fig. 5(c). This also forces the inverters 3 and 4 to operate at lower frequency, thereby increasing their output power. Output power of PV_2 still corresponds to its maximum power of 200kW as observed in Fig. 6(a).

Similarly when the insolation on the second PV source decreases at t=2s, the operating frequency is decreased further to obtain the new equilibrium point, where the PV sources PV_1 and PV_2 operate at their maximum power of 100kW and 60kW(as mentioned in Table 2).
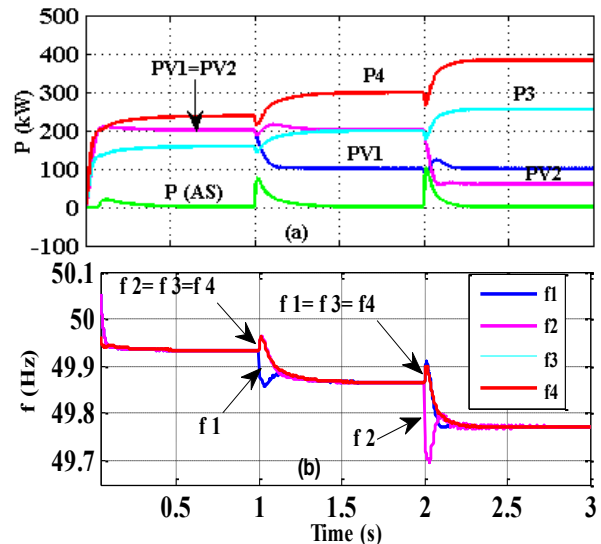
Fig. 6 Results with modified active power droop control and conventional reactive power control Active power (b) Frequency

The remaining active power (640kW) is matched by DG_3 and DG_4 in proportion to their rating. Thus, PV based DGs always extract the maximum possible power from PV arrays and the remaining power is met through the remaining DGs, till they reach their limit (as set by droop settings).Therefore AS remains off in modified droop control as long as the DGs (other than PV based) operate below their limits. AS supplies power only for a short duration (when the step changes in power occur), to minimize the active power mismatch required to ensure stability. Thus, optimum utilization of the various sources is ensured. The reactive power sharing by DGs remains the same as that of Fig. 5(b) as all inverters are controlled using conventional Q-V droop control method.

Similarly when the insolation on the second PV source decreases at t=2s, the operating frequency is decreased further

to obtain the new equilibrium point, where the PV sources PV_1 and PV_2 operate at their maximum power of 100kW and 60kW(as mentioned in Table 2). The remaining active power (640kW) is matched by DG_3 (260kW) and DG_4(387kW) in proportion to their rating(i.e. in ratio 375kkVA:565kVA or 1.53:2.23). Thus, PV based DGs always extract the maximum possible power from PV arrays and the remaining power is met through the remaining DGs, till they reach their limit (as set by droop settings).Therefore AS remains off in modified droop control as long as the DGs (other than PV based) operate below their limits. AS supplies power only for a short duration (when the step changes in power occur), to minimize the active power mismatch for ensuring stability. Thus, optimum utilization of the various sources is ensured. The reactive power sharing by DGs remains the same as that of Fig.5 (b) as all inverters are controlled using conventional Q-V droop control method.

The inverters can also be controlled to share the reactive power equally by the inverters as mentioned in equal reactive power sharing (ERPS) approach [20]. The reactive power obtained using ERPS algorithm are used as references Q_1^*, Q_2^*, Q_3^* and Q_4^* (shown by Q^* in Fig. 4) to determine droop characteristics for reactive power sharing. As reactive power demand of load is 600kVAR, all inverters are assigned reference values of 150kVAR. Fig.7 shows that the reactive power delivered by all inverters is about 150 kVAR. The line impedances and their mismatch is the reason for the inaccuracy in the reactive power sharing. It can be minimized by introducing the virtual line impedance in the line [15].
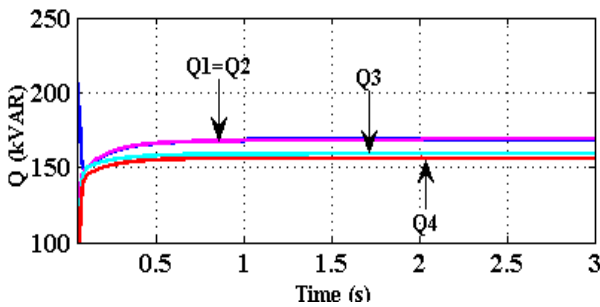
Fig. 7. Reactive power sharing using ERPS approach

It is observed that reactive power assigned to each inverter is nearly independent of the active power delivered by the inverter. The results are also summarized in Table 3. It is observed from the Table 3 that these approaches (reactive power sharing with conventional droop control and ERPS) do not yield the equal percentage utilization of the inverters (referred as utilization factor UF and defined as the ratio of apparent power supplied by the inverter to the nominal apparent power rating). The variation in the *UF* of the inverters is large leading to higher standard deviation of *UF*. This can be minimized by assigning higher reactive power to the PV based inverters that supply relatively lesser active power.

Figure 8 shows results of power sharing using the proposed modified active and reactive droop control, which not only extracts the maximum power from the PV array but also tries to achieve the equal *UF*s of the inverters. Figure 8(a) shows active power sharing which is similar to that shown in Fig.6 (a). Figure 8(b) shows reactive power sharing obtained using proportional apparent power sharing (PAPS) algorithm to achieve equal *UF*s of inverters. During t=0-1s, when both the PV based inverters of 250kVA capacity supply 200kW, the reactive power supplied by them is very less (10kVAR as shown in Table 3). However, at t=1-2s when the output power of PV_1 decreases to 100kW, reactive power supplied through inverter-1 is increased (155kVAR). This in turn reduces the reactive power supplied through inverters 3 and 4(245kVAR and 360kVAR to 180kVAR and 200kVAR). Similarly, when the output power of PV_2 decreases to 60kW at t=2s, reactive power supplied through inverter-2 increases as observed in Fig. 8 and Table 3. Hence, reactive power supplied by inverters 3 and 4 further reduces.
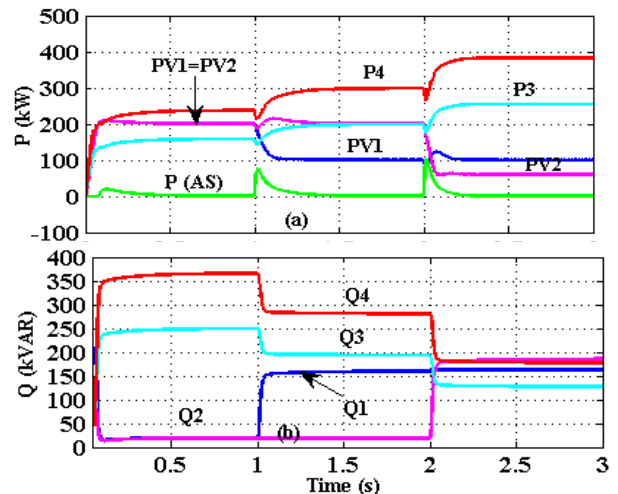
Fig. 8. Simulation results with proposed active-reactive power control approach: (a) Active power of DGs (b) Reactive power of DGs

The conventional droop control gives nearly equal *UF*s (around 71%, 59% and 50% for t=0-1s, 1-2s and 2-3s respectively) for all the inverters, however at the cost of inefficient operation caused due to the operation of the PV sources away from their MPPs. The modified droop control along with conventional reactive power droop control or ERPS minimizes the capacity of AS. But the *UF*s of the inverters vary greatly as observed in Table 3. It is also observed that some of the inverters may operate above or near to their limits (Inverter 1 till t=1s and Inverter 2 till t=2s as observed from Table 3). In the proposed control strategy, as the reactive power shared by each inverter is assigned based on the available apparent power rating of the inverters, effective utilization of the inverters is ensured. As a result, variation in the *UF*s and hence, the *SD* of the *UF*s are

relatively low for the proposed strategy as mentioned in Table 3.

To illustrate the performance of the proposed control strategy when operating with heavy and low load conditions, two cases are considered whose results are presented in form of Figs. 9 and 10, respectively.

Table 3 Active and reactive power sharing amongst DGs and their utilization factor for various control approaches

t (s)	Inv No	Conventional droop control				Modified active/Conventional reactive droop control					Modified active/ERPS droop control					Modified active/PAPS droop control				
		P_i	Q_i	S_i	UF	P_i	Q_i	S_i	UF	SD	P_i	Q_i	S_i	UF	SD	P_i	Q_i	S_i	UF	SD
0 to 1	1	140	108	177	71	200	108	250	91		200	160	256	102		200	10	200	80	0.01
	2	140	108	177	71	200	108	250	91		200	160	256	102		200	10	200	80	
	3	215	160	268	71	167	160	375	62	0.17	167	155	228	60	0.26	167	245	297	79	
	4	312	240	394	70	248	240	565	61		248	155	292	51		248	360	437	77	
1 to 2	1	100	108	147	59	100	108	147	59		100	160	189	75		100	155	184	74	
	2	100	108	147	59	200	108	227	91		200	160	256	102	0.17	200	10	200	80	0.04
	3	160	160	226	60	203	160	258	69	0.13	203	155	255	68		203	180	271	72	
	4	235	240	336	59	305	240	388	69		305	155	342	60		305	280	414	73	
2 to 3	1	60	108	126	49	100	108	147	59		100	160	189	75		100	160	189	75	
	2	60	108	126	49	60	108	124	49	0.16	60	160	171	68	0.05	60	160	171	68	0.03
	3	100	160	189	50	260	160	305	81		260	155	303	81		260	125	288	76	
	4	155	240	286	51	387	240	455	81		387	155	417	74		387	180	427	75	
Note: P_i, Q_i, S_i are mentioned in kW, kVAR and kVA. UF is mentioned in percentage.																				

(b) Reactive power sharing (c) Frequency

At t=1s, the reduction in the active power of PV based DGs is compensated by the increase in the active power

Fig. 9(a) shows that both the PV based DGs supply 200kW (corresponding to 1kW/m²) till t=1s and then supply 100kW (corresponding to 0.5kW/m²). Till t=2s the total load to be supplied is 721kVA at 0.8pf (600kW, 400kVAR). A step change in load is considered at t=2s resulting in the total load of 1220kVA at 0.8 pf lag (1000kW, 700kVAR).
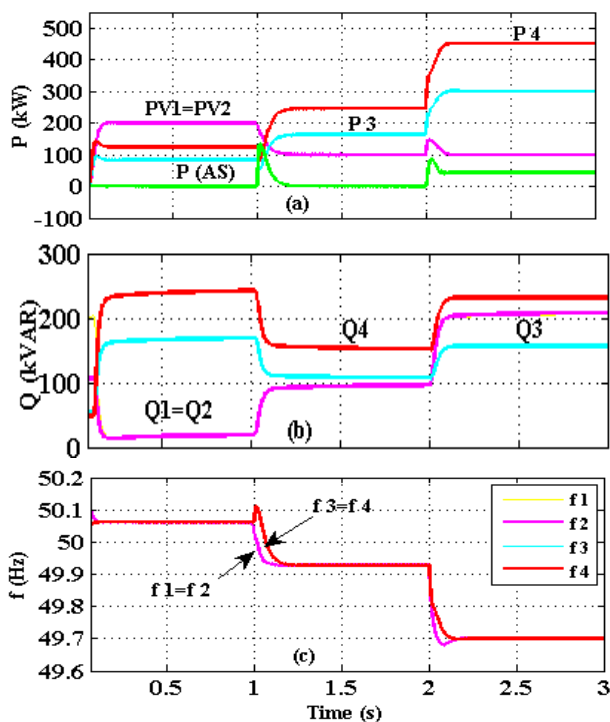
Fig.9. Performance with heavy load: (a) Active power sharing

supplied through inverters 3 and 4. They share the active power in proportion to their ratings. This is achieved by quickly lowering the operating frequency as observed in Fig. 9(c). As the active power demand is well below the total active power generating capacity of all the DGs put together, the output power of AS is zero. Just like earlier case, the decrease in the active power of the DG₁ and DG₂ causes their reactive power to increase. At t=2s, the active power demand of the load increases to a level at which the DG₃ and DG₄ reach to their active power limit. The active power limit for the DG₃ and DG₄ are set as 300kW and 450kW, respectively. Thus, DG₁–DG₄ can supply only 950kW, forcing the AS source to provide the deficit active power (50kW). When the total active powers of the DG₁–DG₄ just match the active power demand of the load, the operating frequency reaches to the least value of 49.7Hz (as set on the droop characteristic). At this point, it is not possible for DG₃ and DG₄ to supply more active power (as already operating on the limits) by further reducing the frequency as per the droop control principle. Hence, any further increase in active power demand is met by increasing the output of AS.

Figure 10 shows results when operating with light load conditions (400kW, 300kW).During t=0-1.5s, PV based DGs

are able to match the active power needed by the load and hence, the DG$_3$ and DG$_4$ do not supply any active power. The operating frequency under this case corresponds to the highest value of 50.2Hz (on the droop characteristic). Under this condition, DG$_3$ and DG$_4$ provide the reactive power just needed by the load. At t=1.5s, the reduction in the insolation level lowers the active power of DG$_1$ and DG$_2$. The modified controller quickly lowers the frequency to a new operating point so that the decrease in the active power of DG$_1$ and DG$_2$ can be matched by the increase in the active power of DG$_3$ and DG$_4$.
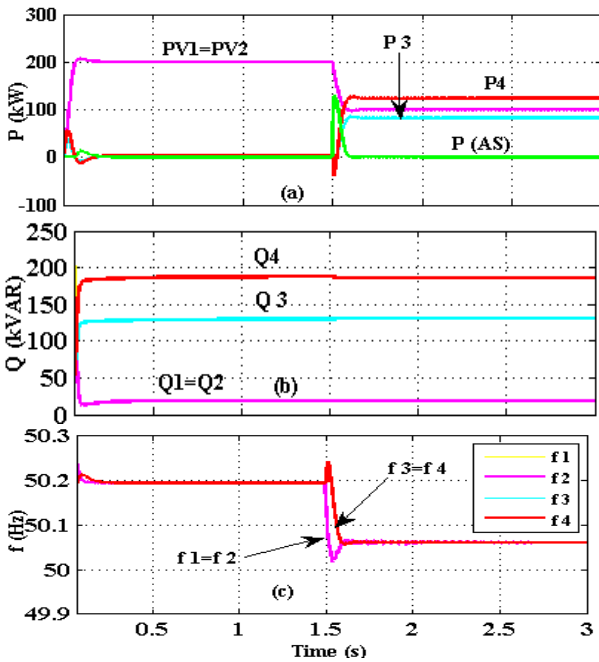
Fig.10. Performance with light load: (a) Active power sharing (b) Reactive power sharing (c) Frequency

Figure 11 shows the performance when the communication link between PSU and SCU fails. The communication between PSC and SCU breaks at t=0.5s and the healthy condition is restored at t=1.5s. When the communication between PSU and SCU gets disturbed, the provisional control by master-slave approach is activated.
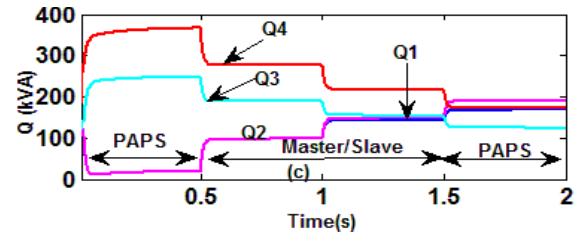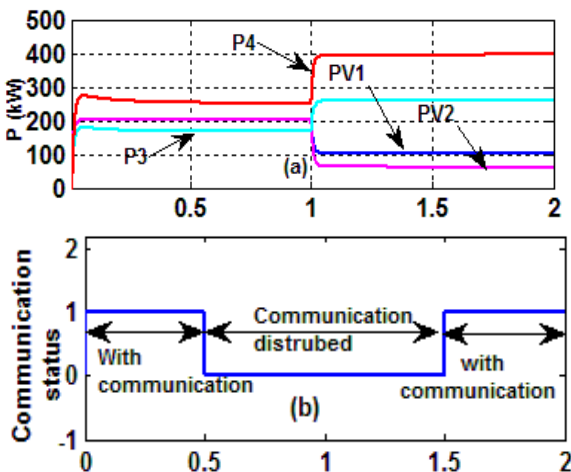
Fig.11. Results with PAPS and master-slave method: (a) Active power sharing (b) Status of communication and (c) Reactive power sharing

Once communication is retrieved, the reactive power references are once again derived through the PAPS algorithm. Fig. 11(a) shows that the active power generated by both the PV sources is PV$_1$=PV$_2$=200kW till t=1s and after t=1s the output of PV sources is reduced to PV$_1$=100 kW and PV$_2$=60kW. Fig. 11(b) shows the status of communication link. The reactive power sharing during healthy and faulty conditions of the communication link is shown in Fig. 11(c) and summarized through the data presented in Table 4.

Table 4 Power sharing with healthy and unhealthy communication link

Time (t)	P$_i$	Q$_i$	S$_i$	S$_N$	UF	SD	Control
0-0.5 s	200	9	200	250	80	0.013	PAPS
	200	9	200	250	80		
	167	240	292	375	78		
	248	357	434	565	77		
0.5-1 s	200	80	215	250	86	0.103	Master - Slave
	200	80	215	250	86		
	167	180	246	375	65		
	248	275	370	565	66		
1-1.5s	100	124	159	250	63	0.086	Master - Slave
	60	131	143	250	57		
	260	145	298	375	79		
	395	215	450	565	79		
1.5-2s	100	157	186	250	74	0.010	PAPS
	60	174	184	250	74		
	260	117	285	375	76		
	395	167	428	565	76		

Note: P$_i$, Q$_i$, S$_i$ are in kW, kVAR and kVA. UF is mentioned in percentage.

It is observed that SD of UF when operating with PAPS algorithm (under healthy conditions i.e. with communication link) is very less. The SD of UF with the master-slave control (when communication link fails) increases manifolds. However, still the performance is much better than that with the schemes like ERPS, conventional droop control, ORPS etc.

5. Conclusion

The conventional droop control does not take into account the variation in the output of the PV based DGs and hence

leads to ineffective utilization of PV sources as well as other DGs. The proposed control strategy modifies the *P-ω* characteristics by quickly adjusting the frequency reference for the PV based DGs such that the decrease in their output power is quickly compensated by the increase in the output power of other DGs. It is observed that the operating frequency is strictly maintained within the predefined limits of 49.7Hz-50.2Hz. The PAPS algorithm used for assigning the reference reactive power to the *Q-V* droop forces the inverter carrying more active power to supply lesser reactive power and vice-versa. It helps in preventing overloading of the inverters. Also, the percentage utilization factors of the inverters are nearly equal as confirmed through the very low value of standard deviation of the utilization factors. Even during the case of communication failure, when the PAPS algorithm is not able to supply the reactive power references to the PCU, reasonably satisfactory performance is guaranteed as the reactive power references are derived locally using master-slave control approach. The AS supplies the energy only when the conventional DGs are unable to provide any extra active power or in case of momentary active power imbalance caused by the sudden change in the power from DGs or change in load. The AS inherently helps in providing stability against sudden power mismatch. The proposed active and reactive power sharing approach can (i) extract the maximum power from PV sources, (ii) minimize the energy drawn from auxiliary source, (iii) provide lower value of standard deviation of utilization factors, (iv) avoid chances of overloading or operating near limits (v) provide dynamic response and (vi) perform even when communication failure occurs. Thus, it offers an effective solution for the optimal utilization of the DGs and the inverters.

References

[1] M. Monfared, S. Golestan, "Control strategies for single-phase grid integration of small-scale renewable energy sources," *A review, Renewable Sustainable Energy Rev.* vol. 16, no.7, pp. 4982-4993, April 2012.

[2] M. Kamran, M. Fazal, M. Mudassar, Shah Rukh Ahmed, et al. "Solar Photovoltaic Grid Parity: A Review of issues, challenges and status of different PV Markets" International journal of renewable energy research, vol.9, no.1 pp.244-260, March 2019.

[3] Q. Zhong, "Robust droop controller for accurate proportional load sharing among inverters operated in parallel," *IEEE Trans. Ind. Electron.,* vol. 60, no.4, pp. 1281–1290, April 2013.

[4] E. Barklund, N. Pogaku, M. Prodanovic, C. H. Aramburo, and T. C. Green, "Energy management in autonomous microgrid using stability-constrained droop control of inverters," *IEEE Trans. Power Electron.,* vol. 23, no. 5, pp.2346-2352, Sep. 2008.

[5] D. Rekioua , T. Rekioua, Y. Soufi, "Control of a grid connected photovoltaic system," IEEE International Conference on Renewable Energy Research and Applications (ICRERA), pp. 1382 - 1387, 22-25 November 2015.

[6] J. Zhang , D.Guo,F.Wang,Y. Zuo, H. Zhang, "Research on energy management strategy for islanded microgrid based on hybrid storage device" IEEE International Conference on Renewable Energy Research and Application (ICRERA) pp. 91 – 96, 20-23 Oct. 2013.

[7] L. Paragond , C. Kurian , B. Singh, " Design and simulation of solar and wind energy conversion system in isolated mode of operation" IEEE International Conference on Renewable Energy Research and Applications (ICRERA),pp.999- 1004,22-25 November 2015.

[8] N. Shah, U. Patel, H. Patel, "Improved reactive power management strategy for photovoltaic based distributed generators" International journal of renewable energy research, vol.8, no.4 pp.2035-2046, Dec. 2018..

[9] Y. Han, H. Li, P. Shen, E .A .A. Coelho, J.M. Guerrero. "Review of active and reactive power sharing strategies in hierarchical controlled microgrids*," IEEE Trans. on Power Electron.*, vol. 32, no.3, pp. 2427- 2451, March 2017.

[10] P. Stumpf , I. Nagy , I. Vajk, "Novel approach of microgrid control," IEEE International Conference on Renewable Energy Research and Applications (ICRERA), pp. 859 -864, 19-22 October 2014.

[11] W. Ferreira de Souza, M. Severo-Mendes, L. Lopes, "Power sharing control strategies for a three-phase microgrid in different operating condition with droop control and damping factor investigation," *IET Renew. Power Gener.*, vol. 9, no. 7, pp. 831–839, Aug. 2015.

[12] W. Cao, H. Su, J. Cao, J. Sun and D. Yang "Improved droop control method in microgrid and its small signal stability analysis," IEEE International Conference on Renewable Energy Research and Application (ICRERA), pp.197-203, 19-22 October 2014.

[13] A. Egwebe, M. Fazeli, P. Ignic, P. Holland "Implementation and stability study of dynamic droop in islanded microgrid," *IEEE Trans. on Energy Conversion,* vol. 31, no.3, pp. 821-831, Sept.2016.

[14] H. Liu, Y. Yang, X. Wang, P. C. Loh, F. Blaabjerg, W. Wang, D. Xu. "An enhanced droop control scheme for resilient active power sharing in paralleled two-stage PV inverter system," in p*roc. IEEE, Applied Power Electro. Conf. and Exposition (APEC),*2016, pp.1253-1260.

[15] H. Mahmood, D. Michaelson and J. Jiang, "Reactive power sharing in islanded microgrids using adaptive voltage droop control," *IEEE Trans. Smart Grid.*, vol. 6, no. 6, pp. 3052-3060, Nov. 2015.

[16] D. Chen, A. Luo, J. Zhou, L. S. Bai, and C. M. Tu, "Rapid reactive power control method for parallel inverters using resistive-capacitive output impedance," in *proc. 1st International Future Energy Electronics Conf.(IFEEC)*, 2013, pp. 98-102.

[17] J. Schiffer, T. Seel, J. Raisch and T. Sezi, "Voltage stability and reactive power sharing in inverter-based microgrids with consensus-based distributed voltage control," *IEEE Trans. Control Syst. Technol.,* vol. 24, no. 1, pp. 96-109, Jan, 2016.

[18] A. Micallef, M. Apap, J. Guerrero, and J. Vasquez, "Reactive power sharing and voltage harmonic distortion compensation of droop controlled single phase islanded microgrids," *IEEE Trans. Smart grid*, vol. 5, no. 3, pp. 1149-1158, May 2014.

[19] J. Yanga, W. Yuana , Y. Suna, et al. "A novel quasi-master-slave control frame for PV-storage independent microgrid," Elsevier journal of Electrical Power and Energy Systems, vol. 97, pp. 262-274,2018.

[20] A. Milczarek, M. Malinowski, J. Guerrero, "Reactive power management in islanded microgrid—proportional power sharing in hierarchical droop control," *IEEE Trans. Smart grid*, vol. 6, no. 4 pp. 1631-1638,July 2015.

[21] Z. Wang. K. Passino, J. Wang, "Optimal reactive power allocation in large scale grid connected photovoltaic system," Journal of optimization theory and application, vol 167, no. 2, pp. 761-779, Nov. 2015.

[22] U. Patel, H. Patel, "Power sharing strategy for photovoltaic Based distributed generators operating in parallel," *Proc .Int. Conf. on Environment and Electrical Engineering*, Florence, Italy, pp. 2040-2045, 2016.

[23] U. Patel, N. Shah, H. Patel, "Reactive power management strategy for photovoltaic based distributed generators operating under non- uniform conditions," *IEEE Int. Conf. on Power Energy, Env. & Intelligent Control (PEEIC)*, Delhi, India, April 14-15, 2018.